GRMHD SIMULATIONS OF JET FORMATION WITH RAISHIN

Y. Mizuno[1], D. H. Hartmann[2], K.-I. Nishikawa[3], S. Koide[4], P. Hardee[5], and G. J. Fishman[6]

[1]*National Space Science and Technology Center, 320 Sparkman Drive, VP 62, Huntsville, AL 35805, USA*
[2]*Kinard Laboratory of Physics, Clemson University, Clemson, SC 29634-0978, USA*
[3]*National Space Science and Technology Center, 320 Sparkman Drive, VP 62, Huntsville, AL 35805, USA*
[4]*Department of Physics, Kumamoto University, Kurokami, Kumamoto, 860-8555, Japan*
[5]*Department of Physics and Astronomy, The University of Alabama, Tuscaloosa, AL 35487, USA*
[6]*NASA-Marshall Space Flight Center, NSSTC, 320 Sparkman Drive, VP 62,Huntsville, AL 35805, USA*

ABSTRACT

We have developed a new three dimensional general relativistic magnetohydrodynamic (GRMHD) code, RAISHIN, using a conservative, high-resolution shock capturing scheme. Numerical fluxes are calculated using the Harten, Lax, & van Leer (HLL) approximate Riemann solver scheme. The flux-interpolated, constrained transport scheme is used to maintain a divergence-free magnetic field. We describe code performance on some test problems in both special and general relativity. Our new GRMHD code has proven to be accurate to second order and has successfully passed several numerical test problems including highly relativistic and magnetized tests in both special and general relativity. We have performed several simulations of non-rotating and rotating black hole systems with a geometrically thin accretion disk. The simulations show the formation of jets driven by the Lorentz force and the gas pressure. It appears that the rotating black hole creates an additional faster, and more collimated outflow inside a broader, slower outflow that is also generated by the rotating accretion disk around a non-rotating black hole. The kinematic jet structure could thus be a sensitive function of black hole rotation.

Key words: general relativity, MHD, simulation, astrophysical jets.

1. INTRODUCTION

Both magnetic and gravitational fields play important roles in the evolution of properties of matter in many astrophysical objects. In highly conducting plasma, the magnetic field can be amplified by gas contraction or shear motion. Even when the magnetic field is weak initially, the magnetic field grows on short time scales and influences the gas dynamics of the system. This is particulary important for a compact object, such as a black hole or a neutron star. Relativistic jets have been observed or postulated in various astrophysical sources, including active galactic nuclei (AGNs) [1, 2], microquasars in the Galaxy [3] and gamma-ray bursts (GRBs) [4, 5, 6]. Promising mechanisms for producing relativistic jets involve magnetohydrodynamic centrifugal acceleration from an accretion disk around the compact object [7], or the extraction of rotational energy from the rotating black hole [8]. In addition, differential rotation of plasma in the disk may lead to magnetorotational instability (MRI), which plays an important role for the transport of angular momentum due to the associated turbulence in accretion disks [9].

Our previous GRMHD code developed by Koide was successfully applied to many high-energy astrophysical phenomena [10, 11, 12, 13, 14, 15]. However, that code cannot perform calculations in highly relativistic or highly magnetized regimes. The critical problem of the previous GRMHD code is that it cannot guarantee a divergence-free magnetic field. Although we introduced a divergence-cleaning step in the code, it cannot reliably follow long-term evolution, except in special cases. In order to overcome these numerical difficulties, we have developed a new, three-dimensional, GRMHD code called RAISHIN, for RelAtIviStic magnetoHydrodynamic sImulatioN. (RAISHIN is the ancient Japanese god of lightning.) It uses a conservative, high-resolution shock capturing scheme.

2. THE RAISHIN CODE

Our GRMHD code, described in greater detail in Mizuno et al. [16], employs conservative schemes to solve the three-dimensional GRMHD equations on uniform and non-uniform grids in each spatial direction. The numerical fluxes are calculated using the Harten, Lax, & van Leer (HLL) approximate Riemann solver scheme. The flux-interpolated, constrained transport scheme is used to maintain a divergence-free magnetic field. In order to examine the numerical accuracy and the numerical efficiency, the code uses four different reconstruction methods: piecewise linear methods with Minmod and MC

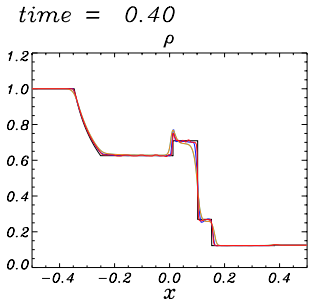

Figure 1. Simulation results of Balsara test 1 at time $t = 0.4$ using the MC slope limiter (blue), the minmod slope limiter (light-blue), CENO (orange) and PPM (red) reconstructions. The black lines are the exact solutions. The results are composed of a left-going fast rarefaction, a left-going slow shock, a contact discontinuity, a right-going slow shock, and a right-going fast rarefaction.

slope-limiter function, convex essentially non-oscillatory (CENO) method, and piecewise parabolic method (PPM) using multistep TVD Runge-Kutta time advance methods with second and third-order time accuracy. To calculate primitive variables from conserved variables, we include two methods, Koide's 2D method and Noble's 2D method.

3. RELATIVISTIC MHD SHOCK-TUBE TEST

Shock-tube tests are the most basic test problems for MHD (HD) codes. Large sets of test-problems in relativistic MHD have been investigated over the years [17]. In some test problems the exact solution of the Riemann problem in relativistic MHD has been calculated by Giacomazzo & Rezzolla [18].

We perform eight simulations of $B^x \neq 0$ cases with exact solutions obtained by Giacomazzo & Rezzolla [18]. Therefore we can compare the simulation results with the exact solutions directly. All tests start with discontinuous initial data at $x = 0$ (see Table 1 in [16]) and with homogenous profiles on either side in Cartesian coordinates. We simulate from $t = 0$ to $t = t_{\rm final}$ with different reconstruction schemes. The fluid satisfies a Γ-law EOS. In all cases we use 400 computational zones with a Courant factor of 0.5.

The result for Balsara Test 1 shown in Fig 1 exhibit good agreement with the exact solution. However, some small discontinuities and large shocks cannot be resolved exactly. This means that we need more computational zones to resolve all small discontinuities and large shocks exactly. Generally, the minmod slope limiter and CENO reconstructions are more diffusive than the MC slope limiter and PPM reconstructions because of the properties of the minmod function. On the other hand, although the MC slope limiter and PPM reconstructions can resolve sharp discontinuities well, some small oscillations are seen at the discontinuities. The PPM reconstruction detects the discontinuities most accurately.

Our previous GRMHD code [12] could not handle some of the extreme cases of relativistic MHD shock-tube tests shown in Table 1 of [16], such as Kommissarov: Shock-Tube test1, Balsara Test2 and Balsara Test3 for large discontinuities of the pressure and magnetic field, Kommissarov: Collision Test and Balsara Test3 for the highly relativistic flow even using different recovery methods such as the Noble 2D method. However the new GRMHD code successfully handles all relativistic MHD shock-tube tests. Therefore the new GRMHD code can operate in a regime with large discontinuities of physical quantities (4 orders of magnitude difference of pressure in Komissarov: Collision Test and Balsara Test3), strong magnetic field ($\beta < 0.004$ and $\sigma > 570$ in Balsara Test 3, where $\beta = p_{gas}/p_{mag}$ and $\sigma = 2p_{mag}/\rho$) and highly relativistic flow ($\gamma > 22$ in Balsara Test4). Handling the regimes of high Lorentz factor and of high magnetization depends on the schemes used to solve the GRMHD equations.

4. 2D GRMHD SIMULATIONS OF JET FORMATION

As a first application, we consider the evolution of a geometrically thin disk with a global magnetic field around a black hole [19].

Recently, in order to investigate the properties of accretion flows onto a black hole associated with the magneto-rotational instability (MRI) [9], many simulations have been performed using a thick torus-like disk with weak poloidal magnetic fields in a torus [20, 21]. The initial "poloidal-loop" magnetic fields in the torus contribute to the generation of MRI, diffusion of matter and magnetic field, and jet generation. However, in their simulations the structure of magnetic fields that piled up and twisted near the black hole is different from the magnetic fields which are twisted by a thin Keplerian disk and/or the frame-dragging effect of the rotating black hole with a stronger initial vertical magnetic field [10, 11, 14]. In the thin disk simulations MRI does not grow since the wavelength at the maximum growth rate is larger than the height of the thin disk. Koide et al. [11] have found that jets are formed from thin Keplerian disks for both counter- and co-rotating black holes. In the co-rotating disk case, the jet had a two-layered structure: an inner gas pressure-driven jet, and an outer magnetically driven jet.

In order to study the formation of relativistic jets from a geometrically thin Keplerian disk, we use a 2.5-dimensional GRMHD code with Boyer-Lindquist coordinates (r, θ, ϕ). In our present simulations: a geometrically thin Keplerian disk rotates around a black hole (non-rotating, $a = 0.0$ or co-rotating, $a = 0.95$), where the disk density is 100 times higher than the coronal density. The background corona is free-falling into the black hole (Bondi flow). The initial magnetic field is assumed to be

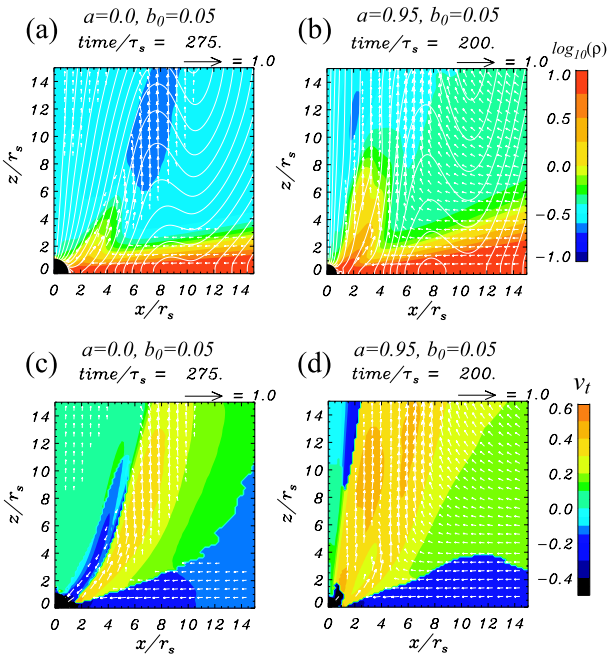

Figure 2. Snapshots of density and total velocity of the non-rotating black hole case ($a = 0.0$; a, c) and the rapidly rotating black hole case ($a = 0.95$; b, d) at the applicable terminal simulation time. The color scales show the logarithm of density (upper panels) and total velocity (lower panels). A negative velocity means inflow towards the black hole. The white lines indicate magnetic field lines. Arrows depict the poloidal velocities normalized to light speed.

uniform and parallel to the rotational axis (We use B_0 as a parameter for magnetic field strength $B_0 = 0.05\sqrt{\rho_0 c^2}$). These initial conditions are the same as [10] and [11] (except for the initial magnetic field strength).

The simulations are performed in the region $1.1r_{\rm S} \leq r \leq 20.0r_S$ (non-rotating black hole case) and $0.75r_S \leq r \leq 20.0r_S$ (rapid rotation black hole case) and $0.03 \leq \theta \leq \pi/2$ with 128×128 computational zones. We assume axisymmetry with respect to the z-axis and mirror symmetry with respect to the equatorial plane. We employ a free boundary condition at the inner and outer boundaries in the radial direction.

Figure 2 shows snapshots of the density and total velocity distribution for the different black hole rotation at each terminal simulation time ($t = 200, 275\tau_S$ where $\tau_S \equiv r_{\rm S}/c$).

The numerical results show that matter in the disk loses angular momentum through the magnetic field and falls into the black hole. A centrifugal barrier decelerates the falling matter and makes a shock around $r = 2r_{\rm S}$. The matter near the shock region is accelerated by the $\mathbf{J} \times \mathbf{B}$ force and the gas pressure increased by the shock, resulting in jet formation. These results are similar to the previous work of several authors [10, 11, 14]. The jets propagate outward through the outer boundary of the simulation region and matter is supplied continuously from the accretion disk. The jets in both cases have velocities somewhat greater than $0.4c$. In the rapidly rotating black hole case the velocity distribution reveals a two-component jet. The outer jet is similar to that of the non-rotating black hole case but the inner jet is not seen in the non-rotating black hole case. The inner jet is faster than the outer jet (over $0.5c$).

The magnetic field is strongly twisted near the black hole region and propagates outward with the jets as an Alfvén wave. In the non-rotating black hole case the magnetic field is twisted by the rotation of the accreting matter and forms a slower, outer jet. On the other hand, in the rapidly rotating black hole case the magnetic field is mainly twisted by the frame-dragging effect of the rotating black hole rather than the rotation of the accreting matter near the black hole region and forms an additional jet component (inner jet) near the black hole region.

A two component jet structure has also been seen in GRMHD simulations of a black hole co-rotating with a thick torus [20, 21]. One component is a matter-dominated outflow (funnel wall jet) with a mildly relativistic velocity ($\sim 0.3c$) along the centrifugal barrier accelerated and collimated by magnetic and gas pressure forces in the inner torus and the surrounding corona. This formation mechanism and jet are the same as the outer jet seen in our simulations. Therefore the funnel wall jet in [20] is the same as the outer jet in our GRMHD simulations. Their other component is a highly-relativistic Poynting flux dominated jet that is produced from the formation of a large scale radial magnetic field within the funnel. In our simulation, such a highly-relativistic Poynting flux dominated jet is not seen. This is likely caused by the difference in the initial magnetic field configuration. In [20] and [21], there are initial "poloidal-loop" magnetic fields inside the torus. In the simulations, the magnetic field is twisted and expands from the torus as a magnetic tower and fills the funnel region [22]. In the late stage of the simulations a highly-relativistic Poynting flux dominated jet is formed in the low density regions in the funnel. On the other hand, our magnetic field vertically threads the disk and ergosphere initially. The vertical magnetic field near the black hole region is twisted by the frame-dragging effect and forms the inner jet. The inner jet is much denser than the highly-relativistic Poynting flux dominated jet of [20] and [21] because in the inner jet the matter is supplied from the accretion disk and the free-falling corona. While our jets are formed by the same basic mechanisms as in [20] and [21], the different initial magnetic configuration has led to different jet properties and a slower matter dominated jet spine.

5. SUMMARY AND CONCLUSIONS

We have developed a new three-dimensional GRMHD code, RAISHIN, by using a conservative high resolution shock-capturing scheme. The numerical fluxes are calculated using the HLL approximate Riemann solver

scheme. The flux-interpolated, constrained transport scheme is used to maintain a divergence-free magnetic field. Several reconstruction and time advance schemes can be chosen for numerical accuracy and the available computational resources.

We performed several test problems in both special and general relativity. There are significant improvements over our previous GRMHD code [12]. Our new GRMHD code can perform in the regimes of high Lorentz factors ($\gamma > 20$) and high magnetic field ($\sigma > 550$), and in the presence of a large discontinuity in the density, pressure and magnetic field. We have compared the results of several reconstruction schemes. The code is second-order accurate even when we use the higher order reconstruction schemes such as CENO and PPM. Nevertheless, higher-order reconstruction schemes can provide more accurate results for some applications. The PPM reconstruction scheme allows a well-resolved treatment of sharp discontinuities. Handling the regimes of high Lorentz factor and of high magnetization depends on the schemes used to solve the GRMHD equations.

We carried out several simulations of non-rotating and rotating black hole systems with a thin accretion disk. The simulations show the formation of jets driven by the Lorentz force and the gas pressure. It appears that the rotating black hole creates an additional, faster, and more collimated inner outflow inside an outflow generated by the rotating accretion disk found for the non-rotating black hole. Thus, kinematic jet structure could be a sensitive function of the black hole rotation.

The new code has proven to be accurate to second order and has successfully passed numerical test problems including highly relativistic cases, and highly magnetized cases in both special and general relativity. We plan to apply this code to a number of high-energy astrophysical phenomena involving highly relativistic flows or compact objects with strong gravitational fields and magnetic fields.

ACKNOWLEDGMENTS

Y. M. is a NASA Postdoctoral Program fellow at NASA Marshall Space Flight Center. K. N. is partially supported by the National Science Foundation awards ATM-0100997, INT-9981508, and AST-0506719, and the National Aeronautic and Space Administration award NASA-INTEG04-0000-0046 to the Univ of Alabama in Huntsville. P.H. acknowledges partial support by National Space Science and Technology (NSSTC/NASA) cooperative agreement NCC8-256 and NSF award AST-0506666. The simulations have been performed on the IBM p690 at the National Center for Supercomputing Applications (NCSA) which is supported by the NSF and Altix3700 BX2 at YITP in Kyoto University.

REFERENCES

[1] Urry, C. M. & Padovani, P. 1995, PASP, 107, 803

[2] Ferrari, A. 1998, ARAA, 36, 539

[3] Mirabel, I. F. & Rodríguez, L. F. 1999, ARAA, 37, 409

[4] Zhang, B. & Mészáros, P. 2004, Int. J. Mod. Phys., A19, 2385 (astro-ph/0311321)

[5] Piran, T. 2005, Reviews of Modern Physics, 76, 1143 (astro-ph/0405503)

[6] Mészáros, P. 2006, Rep. Prog. Phys., in press (astro-ph/0605208)

[7] Blandford, R. D. & Payne, D. G. 1982,MNRAS, 199, 883

[8] Blandford, R. D. & Znajek, R. L. 1977,MNRAS, 179, 433

[9] Balbus, S. A. & Hawley, J. F. 1998, Rev. Mod. Phys., 70, 1

[10] Koide, S., Shibata, K. & Kudoh T. 1999, ApJ, 522, 727

[11] Koide, S., Meier, D. L., Shibata, K., & Kudoh, T. 2000, ApJ, 536, 668

[12] Koide, S. 2003, Phys. Rev. D, 67, 104010

[13] Koide, S., Kudoh, T., & Shibata, K. 2006, Phys. Rev. D, 74, 044005

[14] Nishikawa, K.-I., Richardson, G., Koide, S., Shibata, K., Kudoh, T., Hardee, P., & Fishman, G. J. 2005, ApJ, 625, 60

[15] Mizuno, Y., Yamada, S., Koide, S., & Shibata, K. 2004, ApJ, 606, 395

[16] Mizuno, Y., Nishikawa, K.-I., Koide, S., Hardee, P., & Fishman, G. J. 2006a, ApJS, submitted (astro-ph/0609004)

[17] Balsara, D. 2001, ApJS, 132, 83

[18] Giacomazzo, B. & Rezzolla, L. 2006, J. Fluid Mech., 562, 223

[19] Mizuno, Y., Nishikawa, K.-I., Koide, S., Hardee, P., & Fishman, G. J. 2006b, in preparation

[20] Hawley, J. F., & Krolik, J. 2006, ApJ, 522, 727

[21] McKinney, J. C. 2006, MNRAS, 368, 1561

[22] Hirose, S., Krolik, J., De Villiers, J. P., & Hawley, J. F. 2004, ApJ, 606, 1083